



Cite this: *Food Funct.*, 2025, **16**, 885

## Application of a dynamic colonic gastrointestinal digestion model to red wines: a study of flavanol metabolism by the gut microbiota and the cardioprotective activity of microbial metabolites†

Juana I. Mosele,<sup>a,b</sup> Blanca Viadel,<sup>c</sup> Silvia Yuste,<sup>a,d</sup> Lidia Tomás-Cobos,<sup>c</sup> Sandra García-Benlloch,<sup>c</sup> María-Teresa Escribano Bailón,<sup>d</sup> Ignacio García Estévez,<sup>d</sup> Pilar Moretón Fraile,<sup>f</sup> Fernando Rodríguez de Rivera,<sup>f</sup> Soledad de Domingo Casado<sup>f</sup> and María-José Motilva <sup>d,\*a</sup>

Over the last decade, research has emphasized the role of the microbiome in regulating cardiovascular physiology and disease progression. Understanding the interplay between wine polyphenols, the gut microbiota, and cardiovascular health could provide valuable insights for uncovering novel therapeutic strategies aimed at preventing and managing cardiovascular disease. In this study, two commercial red wines were subjected to *in vitro* dynamic gastrointestinal digestion (GIS) to monitor the flavanol–microbiota interaction by evaluating the resulting microbial metabolites. Furthermore, the cardiovascular protective activity of wine flavanol microbial metabolites was investigated, integrating their effects on antihypertensive activity, cholesterol metabolism and insulin resistance into human endothelial (EA.hy926) and hepatic (HepG2) cell lines. A significant production of microbial flavanol metabolites, with a prevalence of phenylpropionic and phenylacetic acids, valerolactones and short chain fatty acids such as butyric acid, was observed, particularly in the transverse and descending colon sections. Incubating HAECS and HepG2 cells with the colon improved cardioprotective parameters. Specifically, an increase in the vasodilator NO, an improvement in the LDL receptors and the HMGCoA enzyme, with positive effects on cholesterol metabolism, and the reduction of glycogen levels improving insulin resistance were observed.

Received 6th August 2024,  
Accepted 26th November 2024

DOI: 10.1039/d4fo03774j

rsc.li/food-function

## 1. Introduction

Wine differs from other alcoholic beverages due to its heterogeneous (poly)phenol content, among which flavanols are prominent components.<sup>1</sup> In wine, flavanols are present as monomers (catechin, epicatechin and epigallocatechin) and proantho-

cyanidin oligomers or polymers exhibiting varying degrees of polymerization according to the structural monomeric units.<sup>1</sup> Beyond imparting sensory and preservative attributes,<sup>2,3</sup> moderate consumption of wine containing flavanols has been associated with the prevention of cardiovascular disease (CVD).<sup>4</sup>

(Poly)phenol bioactivity hinges on their bioavailability. While monomers of flavanols are partially absorbed in the small intestine during gastrointestinal digestion, intact proanthocyanidins do not undergo absorption.<sup>5</sup> After gastrointestinal absorption, subsequent biomodifications of flavanol monomers occur, particularly in the liver, yielding diverse sulphated, glucuronidated, and methylated phase-II conjugated metabolites.<sup>5,6</sup> Some conjugated metabolites re-enter the enterohepatic recirculation, reaching the colon together with non-absorbed flavanols. Within the gut, microbial action catalyzes transformations such as dehydroxylation, demethylation, ring fission and decarboxylation, generating low molecular weight compounds, such as phenolic acids, phenyl-valerolactones and phenyl-valeric acids.<sup>5,7</sup> These colonic catabolites can be absorbed by colonocytes, increasing the overall bioavailability of flavanols and diversifying the spectrum of bio-

<sup>a</sup>Instituto de Ciencias de la Vid y del Vino-ICVV (Consejo Superior de Investigaciones Científicas-CSIC, Universidad de La Rioja-UR, Gobierno de La Rioja), Finca La Grajera, Ctra. de Burgos Km. 6 (LO-20, - salida 13), 26007 Logroño, Spain. E-mail: motilva@icvv.es

<sup>b</sup>Fisicoquímica, Facultad de Farmacia y Bioquímica-IBIMOL, Universidad de Buenos Aires-CONICET, 1113 Buenos Aires, Argentina

<sup>c</sup>Ainia, Technology Centre, C/Benjamin Franklin 5-11, 46980 Paterna, Valencia, Spain

<sup>d</sup>Antioxidants Research Group, Food Technology Department, Agrotecnic-RECERCA Center, University of Lleida, 25198 Lleida, Spain

<sup>e</sup>Department of Analytical Chemistry, Nutrition and Food Science, Universidad de Salamanca, Campus Miguel de Unamuno s/n, E37007 Salamanca, Spain

<sup>f</sup>Bodegas Pradorey, Real Sitio de Ventosilla SA, Gumiel de Mercado, Burgos, Spain

† Electronic supplementary information (ESI) available. See DOI: <https://doi.org/10.1039/d4fo03774j>

active molecules.<sup>5,7,8</sup> The flavanol catabolites generated by the gut microbiota may exert more biological effect than their parent compounds.<sup>9</sup> Moreover, the interactions between flavanols and the gut microbiota are intricate and reciprocal, influencing microbiome richness, diversity, composition and function.<sup>10,11</sup> Understanding the colonic metabolism and flavanol-gut microbiota interactions is pivotal for unraveling wine-health relationships and identifying molecules potentially involved in CVD prevention.

Therefore, to explore and determine the mechanisms of action of (poly)phenols and their role in disease prevention, it is crucial to understand the factors that constrain their bioactivity. Dynamic *in vitro* models simulating human digestion serve as simple and ethical alternatives for assessing the digestibility, stability, structural changes and bio-accessibility of food bioactive compounds. Multi-compartmental gastro-intestinal simulator (GIS) systems comprise (i) gastric, (ii) duodenal and (iii) jejunal chambers, coupled with a system of trichamber colonic fermentation including the (iv) ascending (AC), (v) transversal (TC) and (vi) descending colon (DC) inoculated with human feces or the gut microbiota. Different studies have applied these dynamic digestion *in vitro* models mimicking the human gut environment to study the two-way interaction between the gut microbiota and phenolic compounds that is pivotal in determining their beneficial effects on human health.<sup>12,13</sup>

Many studies on (poly)phenols to date have focused on the bioactivities of one specific molecule in aglycone form, often at supraphysiological doses, whereas foods contain complex mixtures with multiple additive or interfering activities.<sup>14</sup> In the specific case of wine flavanols, most of the bioactivity studies in cell line models have been carried out with the catechin and epicatechin monomers, omitting the complex mixture of proanthocyanidins that during the gastrointestinal digestion are hydrolysed into monomers, which are subsequently strongly metabolized by the gut microbiota. Therefore, the main objective of this study was to deepen the understanding of the potential cardioprotective effects of colonic metabolites derived from wine flavanols. For this, two commercial Tempranillo red wines (2020 and 2021 harvests) were selected based on their high flavanol contents. The wines were subjected to *in vitro* dynamic GIS to monitor the stability and transformation of flavanols during the gastro-intestinal digestion and to determine the main microbial metabolites produced after their colonic fermentation. Furthermore, the cardiovascular protective activity of wine flavanol microbial metabolites was investigated, integrating their effects on antihypertensive activity, cholesterol metabolism, and insulin resistance into human endothelial (EA.hy926) and hepatic (HepG2) cell lines.

## 2. Materials and methods

### 2.1. Wine samples and determination of flavanol content

Red wines from both the 2020 and 2021 harvests were obtained from *Vitis vinifera* L. cv. Tempranillo grapes by Bodegas Pradorey (Burgos, Spain). Alcoholic fermentation was

performed in stainless steel tanks and malolactic fermentation and ageing were carried out in French oak barrels for 1 year before bottling. Prior to conducting the HPLC-DAD-ESI-MS analysis of flavanols, wines were fractionated using a cationic exchange cartridge (Oasis MCX, Waters Corp., Milford, MA, USA) as previously reported.<sup>15</sup> Chlorogenic acid (Sigma-Aldrich, St Louis, MO, USA) was incorporated into the samples as an internal standard, achieving a final concentration of 0.025 mg mL<sup>-1</sup>. Then, chromatographic separation was achieved using an Agilent 1200 series HPLC system equipped with an Agilent Poroshell 120 EC-18 column (2.7 µm, 4.6 mm × 150 mm) (Agilent Technologies, Waldbronn, Germany), maintained at a temperature of 25° C. The mobile phase was composed of solvent A, 0.1% (v/v) formic acid (VWR International, Fontenay-sous Bois, France) aqueous solution, and solvent B, HPLC grade acetonitrile (Merck KGaA, Darmstadt, Germany). Flavanols were quantified by mass spectrometry using a 3200 QTRAP triple quadrupole mass spectrometer (AB Sciex, USA) equipped with an electrospray ionization source (ESI Turbo V<sup>TM</sup> Source). The detailed conditions of the HPLC and mass spectrometry procedures are provided by García-Estévez *et al.* (2017).<sup>15</sup> Calibration curves for (+)-catechin, (-)-epicatechin, procyanidin dimers B1 and B2, procyanidin trimer C1, (-)-epicatechin 3-O-gallate, (+)-gallocatechin, and (-)-epigallocatechin were utilized for quantification. Monomeric flavanols were purchased from Sigma-Aldrich (St Louis, MO, USA), whereas procyanidin dimers and trimers were purchased from Extrasynthèse (Genay, France). When the corresponding standard was not available, the flavanol was quantified as equivalents of the most related flavanol on the basis of their structure. Thus, procyanidin dimers B3 and B7 were quantified as procyanidin dimer B1 equivalents, procyanidin dimers B4, B5, B6 and B7 were quantified as procyanidin dimer B2 equivalents, procyanidin trimers, tetramers and pentamers were quantified as procyanidin trimer C1 equivalents and prodelphinidins were quantified as gallocatechin equivalents. The flavanol composition of red wines from the 2020 and 2021 harvests is detailed in Table 1. The wine flavanol concentration was expressed as mean ± standard deviation (SD) of the average of 3 replicates per wine.

### 2.2. Simulated digestion in the dynamic colonic gastrointestinal digester

The dynamic-colonic gastrointestinal digester (D-CGD) was developed by AINIA Technology Center (Valencia, Spain).<sup>16</sup> The system consists of a computer-assisted model of five interconnected double jacket vessels imitating the physiological conditions of the stomach (G: vessel 1), small intestine (I: vessel 2), and the three colonic sections: the AC (vessel 3), the TC (vessel 4), and the DC (vessel 5) sections (ESI Fig. S1†). All compartments were connected by peristaltic pumps, working semi-continuously in G and I and continuously in the AC, TC and DC sections. The system setup, that is, the volumetric capacity, pH, anaerobiosis (O<sub>2</sub> and CO<sub>2</sub> levels), and temperature (37 °C) were controlled.<sup>16</sup> The pH was continuously controlled in the compartments for the stomach (following pH changes during



**Table 1** Flavanol concentration in red wines from the 2020 and 2021 harvests

Compound (mg L <sup>-1</sup> wine)	2020 wine	2021 wine
Catechin	5.0 ± 0.3	4.7 ± 0.2
Epicatechin	6 ± 1	13.4 ± 0.3
Gallocatechin	1.57 ± 0.09	1.62 ± 0.01
Epigallocatechin	1.01 ± 0.02	1.4 ± 0.1
Epigallocatechin gallate	0.003 ± 2 × 10 <sup>-5</sup>	0.002 ± 2 × 10 <sup>-5</sup>
Epicatechin gallate	0.010 ± 0.001	0.11 ± 0.01
<i>Total flavan-3-ol monomers</i>	13.6 ± 1	21.2 ± 0.6
Procyandin dimer B1	42.3 ± 0.4	29.9 ± 0.4
Procyandin dimer B2	19.5 ± 0.6	16.8 ± 0.6
Procyandin dimer B3	3.3 ± 0.1	4.3 ± 0.1
<i>Total proanthocyanidin dimers</i>	82 ± 2	82 ± 2
<i>Total proanthocyanidin trimers</i>	7.6 ± 0.9	9.0 ± 0.5
<i>Total proanthocyanidin tetramers</i>	3.9 ± 0.2	5.6 ± 0.1
<i>Total proanthocyanidin pentamers</i>	0.36 ± 0.01	0.54 ± 0.01
<i>Total gallocatechins and prodelphinidins</i>	6.4 ± 0.3	7.3 ± 0.3
<i>Total catechins and procyandins</i>	105 ± 7	114 ± 2
<b>Total flavanols</b>	<b>111 ± 8</b>	<b>122 ± 2</b>

Results are expressed as mean ± standard deviation (SD) (n = 3).

gastric digestion, from pH 4.8 to pH 1.7) and the small intestine (pH 6.5–7), using secretions of 1 mol L<sup>-1</sup> hydrochloric acid and 1 mol L<sup>-1</sup> sodium bicarbonate, respectively.<sup>17</sup> Anaerobiosis of the system was achieved by the addition of nitrogen.<sup>16</sup>

**2.2.1. Dynamic gastrointestinal digestion.** The dynamic gastrointestinal digestion consisted of two steps: a gastric digestion (G) (2 h) followed by an intestinal digestion (I) (6 h).<sup>16</sup> Digestion in G was performed by adding a continuous flow of 0.03% (w/v) pepsin (from porcine mucosa, ≥2500 units per g; P7012-56, Sigma-Aldrich, Spain) to a gastric electrolytic solution. The gastric pH medium was set up according to a pH curve observed in *in vivo* data by adding a HCl solution (1 M) (HCl, 37% purity, VWR Chemicals, Spain). After 2 h, the gastric digested material generated was immediately transferred to the I vessel, where simulated digestion was conducted *via* the continuous addition of an intestinal solution consisting of pancreatin (1.9 g L<sup>-1</sup>) (pancreatin P1750-100 G, Sigma-Aldrich, Spain), NaHCO<sub>3</sub> (12 g L<sup>-1</sup>) (Merck, Germany), and Oxgall dehydrated fresh bile (6 g L<sup>-1</sup>, bile bovine, B3883, BD, USA) in distilled water (240 mL for the whole intestinal digestion step). After that, the intestinal digested material generated was immediately transferred to the third vessel (AC) for 30 min, simulating the digestion transfer through the ileocecal valve to the AC. The transferred material was maintained in the whole colonic segment for 76 h under a continuous dynamic flow from the AC entrance to the DC exit, according to Rosès *et al.* (2023).<sup>18</sup>

**2.2.2. Dynamic *in vitro* colonic fermentation.** Fresh feces from 4 healthy adults, non-smokers, with no history of antibiotic use in the previous three months and no background of intestinal disease were collected and transported in special anaerobic bags (BDGasPak<sup>TM</sup> systems) (Becton, Dickinson and Company, NJ, USA). The samples were diluted and regenerated

in a physiological phosphate buffer with thioglycolate 20% (w/v) (Merk, Spain). This mixture was then homogenized in a stomacher and centrifuged at 3000g for 15 min (Heraeus Multifuge x3R Centrifuge, Thermo Scientific, Spain). The supernatant was collected and inoculated in the colon vessels (ESI Fig. S1†) according to Rosès *et al.* (2021).<sup>19</sup> Hence, 50, 80 and 60 mL of the collected supernatant were placed in the AC section, the TC section, and the DC section, respectively, and filled with culture medium<sup>20</sup> of up to a total volume of 1000, 1600 and 1200 mL, respectively, allowing simulation of the conditions of the human colon media.

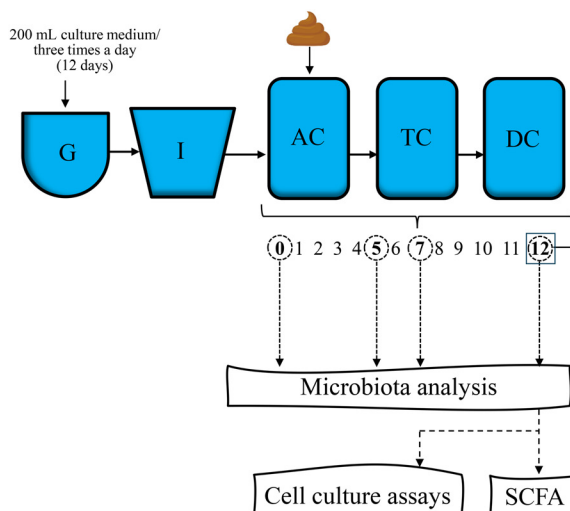
**2.2.3. Experimental protocol: *in vitro* gastrointestinal digestion and colonic fermentation of red wine.** The experimental design and setup are depicted in Fig. 1. The experiment was composed of two different phases. First, a stabilization period of 12 days (days 0–12), where a stable colonic microbiota was reached, followed by a wine treatment period of 14 days (days 13–26), where the microbiota was fed with red wine once per day. For the microbiota stabilization period (day 0 to day 12), 200 mL of the culture medium was added to G three times a day. After the stabilization period and during the wine treatment period (days 13–26), the system was fed with 100 mL of red wine once a day (up to a final volume of 200 mL) and with 200 mL of the culture medium twice a day.<sup>20,21</sup> Samples of the culture media from the three colonic reactors (AC, TC, and DC) were collected at different times during the stabilization (days 0, 5, 7 and 12) and treatment (days 13–16, 18–21, 23 and 26) periods and used for further analysis (Fig. 1).

### 2.3. Analysis of wine flavanols and their microbial metabolites by ultra-high performance liquid chromatography with triple-quadrupole mass spectrometry (UHPLC/QqQ-MS/MS) in the different digestion steps

The monitored wine flavanol transformation during the continuous gastrointestinal digestion and colonic fermentation was conducted through UHPLC-QqQ-MS/MS. Samples (50 mL of media) were collected from each section (Fig. 1) at the end of the stabilization period (day 12) and during the treatment period (days 13, 14, 15, 16, 18, 20, 23 and 26) and stored at –80 °C until analysis. Prior to the chromatographic analysis, the samples were filtered (PTFE syringe filters, 0.22 µm pore size, Scharlab Chemie, Sentmenat, Catalonia, Spain) and analyzed by UHPLC-QqQ-MS/MS based on the method described by Royo *et al.* (2021).<sup>22</sup> Separation of analytes was carried out in a liquid chromatograph (Shimadzu Nexera, Shimadzu Corporation, Japan), coupled to a 3200QTRAP triple quadrupole mass spectrometer (AB Sciex, USA) equipped with an electrospray ionization source (ESI Turbo V<sup>TM</sup> Source). The (poly)phenol separation was performed in a Waters AcQuity BEH C18 column (100 mm × 2.1 mm, 1.7 µm) equipped with a VanGuard<sup>TM</sup> AcQuity BEH C18 pre-column (5 × 2.1 mm, 1.7 µm) (Milford, MA, USA). The electrospray (ESI) interface was used in the negative mode [M – H]<sup>–</sup>. Data acquisition was carried out with the Analyst<sup>®</sup> 1.6.2 software (AB Sciex, USA).



## STABILIZATION PERIOD (0-12 days)



## WINE TREATMENT PERIOD (13-26 days)

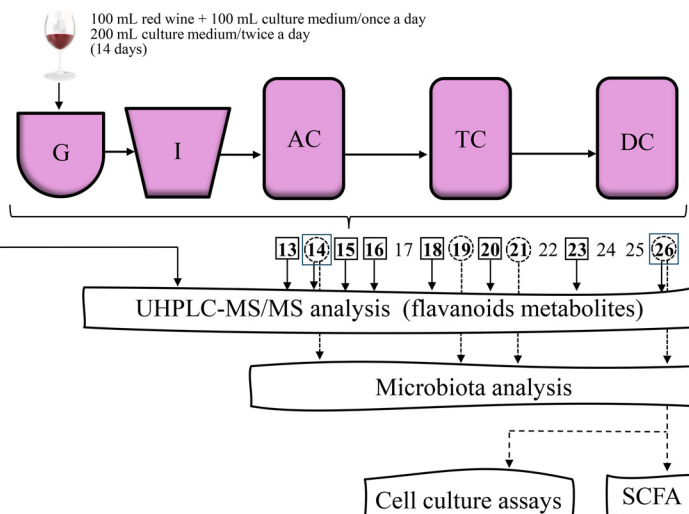


**Fig. 1** Scheme of the experimental protocol of the *in vitro* gastrointestinal digestion and colonic fermentation of red wine. G: gastric digestion step, I: intestinal digestion step, AC: ascending colon section, TC: transversal colon section, DC: descending colon section, SCFA: short chain fatty acid. Bold numbers are the days of sampling media from the reactors during stabilization (0–12 days) and treatment (13–26 days) periods, respectively. The dashed circles indicate the days of sampling media for microbiota analysis during stabilization (days 0, 5, 7, and 12) and treatment (days 14, 19, 21, and 26) periods, and for SCFA and cell culture assays at the end of the stabilization (day 12) and treatment (day 26) periods. The squares indicate the days of sampling media for chromatographic analysis (UHPLC-MS/MS) of flavonoid metabolites at the end of the stabilization period (day 12) and during the treatment period (days 13, 14, 15, 16, 18, 20, 23 and 26).

The wine flavanol metabolites were identified by comparing their spectra and retention times with those of externally injected standards. Compounds for which standards were not available were tentatively identified using MRM transitions with the mass of the parent ion ( $M - H$ ) and typical MS fragmentation pattern described in the literature. Some of the compounds were quantified using the calibration curves of their corresponding commercial standards. The other compounds were tentatively quantified using the calibration curves of standards with similar chemical structures. ESI Table S1† shows the selected reaction monitoring (SRM) conditions, the cone voltage and collision energy and the commercial standard used for quantification. The concentration of the wine flavanols and their microbial metabolites in the gastrointestinal and colon media (AC, TC and DC) was expressed as the mean of the average of two replicates.

The phenol commercial standards used for the identification and quantification were epicatechin and procyanidin B2 (Extrasynthese), procyanidin B1 (Purifa, Dongguan, China), catechin, 4-hydroxybenzoic acid, 4-hydroxyphenylacetic acid, 3,4-dihydroxybenzoic acid (protocatechuic acid), *trans*-coumaric acid, gallic acid and 4,4-bis(4-hydroxyphenyl)valeric acid (Sigma-Aldrich), 5-(3',4'-dihydroxyphenyl)- $\delta$ -valerolactone (TransMIT, Gießen, Germany), 3-(3,4-dihydroxyphenyl)propionic acid and 3,4-dihydroxyphenylacetic acid (Alfa Aesar, Massachusetts, USA), 3-(3-hydroxyphenyl)propionic acid (Biosynth Carbosynth, Compton, United Kingdom), hippuric acid and 3-phenylpropionic acid (Thermo Fisher Scientific, Waltham, MA, USA), catechol (TCI, Tokyo, Japan), pyrogallol

(Glentham Life Sciences, Corsham, United Kingdom) and gallicatechin (Target Mol, Massachusetts, USA). Stock solutions of the standard were prepared in methanol ( $1000 \text{ mg L}^{-1}$ ) and stored at  $-20^\circ\text{C}$ . Methanol (HPLC grade), formic acid (HPLC grade), acetonitrile (HPLC grade) and HCl were purchased from VWR Chemicals BDH Prolabo (Leuven, Belgium). The water was of Milli-Q quality (Millipore Corp., Bedford, MA, USA).

#### 2.4. Microbiota analysis

The microbial population during the stabilization and wine treatment periods was checked by bacterial plate counts. Culture medium samples were collected by duplicate at different days (days 0, 5, 7, and 12) of the stabilization period to monitor the maintenance of microbial populations and at different days during the wine treatment period (days 14, 19, 21 and 26) (Fig. 1). Ten milliliters of media were taken from each colon reactor and serially diluted in saline solution. The plates were inoculated with 1 mL of 4 serial dilutions of the media by duplicate and incubated at  $37^\circ\text{C}$  under aerobic or anaerobic conditions. The following bacterial groups were quantified by the direct plating method on specific colonic culture medium ( $\text{CFU mL}^{-1}$ ): *Lactobacillus* (MRS agar using the MALDI-TOF technique to verify lactobacilli colonies), *Bifidobacterium* (TOS-propionate agar enriched with MUP), *Enterobacter* (VRBD agar), *Clostridium* (TSC agar enriched with cycloserin) and total anaerobic bacteria (Schaedler agar). Results were expressed as  $\log \text{CFU mL}^{-1}$  culture medium.



## 2.5. Determination of short-chain fatty acids (SCFAs)

Culture medium samples were collected in triplicate from each reactor (AC, TC and DC) at the end of the stabilization (day 12) and wine treatment (day 26) periods (Fig. 1). Samples were pooled and filtered (0.2 µm filters) previously for chromatographic analysis. The microbial SCFA acetic, propionic and butyric acids were analyzed by gas chromatography coupled with a flame-ionization detector (GC-FID) after liquid-liquid extraction. Briefly, ethyl acetate containing capric acid as the internal standard (IS) was added to 10 mL of a medium sample collected from each reactor (AC, TC and DC), mixed for 10 min and centrifuged. The supernatant was filtered and injected into a GC-FID instrument (AS 800 C.U., CE Instruments, Wigan, United Kingdom) equipped with an HP-FFAP 25 m × 0.2 mm × 0.33 mm column (Agilent Technologies, Santa Clara, CA, USA). The SCFAs were quantified by interpolation in the calibration curve using capric acid as IS.

## 2.6. Cell culture assays

**2.6.1. Cell cultures.** Human endothelial (EA.hy926) and human hepatic (Hep G2) cell lines (both from the American Type Culture Collection, Manassas, VA, USA) were used as vascular homeostasis and cholesterol and insulin resistance models, respectively, to conduct the functional analysis of wine flavanol colonic metabolites. The cells were cultured in high glucose-DMEM (Sigma-Aldrich, St Louis, MO, USA) supplemented with 10% of fetal bovine serum (Gibco, BRL, Australia) and 1% penicillin-streptomycin at 37 °C under a humidified atmosphere of 5% CO<sub>2</sub>. The medium was changed every 2–3 days until it reached a 90% confluence.

**2.6.2. Preparation of test samples.** Medium culture samples from the DC reactor at the end of the stabilization (day 12) and wine treatment (day 26) periods (Fig. 1), respectively, were collected in triplicate, pooled, and filtered (0.2 µm filters). Each sample was measured, adjusted to 6–8 pH and stored at –20 °C until the subsequent experiments.

**2.6.3. Cell viability assay.** To define the non-toxic levels of microbial wine flavanol metabolites present in the culture medium samples from a DC colon reactor, cell viability was evaluated through a fluori-colorimetric assay. Briefly, 2 × 10<sup>4</sup> cells were seeded in 96-well plates and treated with different serial dilutions from the samples of DC (days 12 and 26) at 37 °C and a 5% CO<sub>2</sub>-humidity environment. After 24 h of treatment, the cell media were replaced with 10% Alamar Blue reagent (Invitrogen, Waltham, MA, USA) in PBS for 2 h and colorimetry was measured using a spectrofluorometer (Fluoroskan, Thermo Fisher Scientific, Waltham, MA, USA) at  $\lambda$  excitation = 540 nm and  $\lambda$  emission = 590 nm. Considering the straight relationship between fluorescence and cellular viability, the equation is as follows:

$$\% \text{ Viability} = (\text{Fluorescence units in the sample} / \text{Fluorescence units in the control}) \times 100.$$

## 2.6.4. Cell treatments

**2.6.4.1. NO and END-1 production.** EA.hy926 cells were seeded in 24-well plates at 1 × 10<sup>5</sup> cells per well. The following day, PBS was depleted from the media and the cells were cultured for 24 h at 37 °C. The cells were then treated for 2 h with a 1/8 dilution of the culture medium samples obtained from the DC colon reactor at day 12 (control media) and at day 26 corresponding to the end of the wine treatment period (media contained microbial wine flavanols) (Fig. 1). After DC media treatment, IL-1b (100 ng mL<sup>−1</sup>) was added and remained overnight. After 24 h, the cell supernatant was collected, and NO was measured using a Griess reagent (Merck, Darmstadt, Germany) and following the manufacturer's protocol. Additionally, EA.hy926 cells were collected for RNA extraction and measurement of the END-1 gene expression.

**2.6.4.2. Cholesterol metabolism.** HepG2 cells were seeded in 12-well plates at 2.5 × 10<sup>5</sup> cells per well. After 24 h, the cells were treated with the DC culture medium samples (from days 12 and 26) (Fig. 1) described above and incubated for 24 h at 37 °C. After the incubation period, the cells were collected for measurement of LDLr and HMGR gene expression (Thermo Fisher Scientific).

**2.6.4.3. Insulin resistance.** To determine the hepatocyte glycogen storage, Hep2 cells were seeded in 12-well plates at 2.5 × 10<sup>5</sup> cells per well. The cells were incubated with 100 mM insulin for 24 h at 37 °C and then the hepatocytes were treated with the DC media samples (from days 12 and 26) (Fig. 1) described above for another 24 h. After this period, the cells were washed three times with PBS and collected for determination of glycogen. The glycogen content in the cells was assayed using an anthrone reagent (Sigma-Aldrich), and the amount of blue compound generated by this reaction was detected on the 620 nm wavelength using a microplate reader (Thermo Fisher Scientific). In addition, the protein content of the collected HepG2 cells was quantified using the BCA method (Thermo Fisher Scientific), and the values were shown as the ratio of glycogen (mg)/protein (mg). Another 12-well plate with the same treatment was collected for measurement of the Akt gene expression (Thermo Fisher Scientific).

**2.6.5. Real time quantitative RT-PCR.** For determination of the gene expression, RNA extraction from different experiments was carried out automatically using the MAXWELL equipment (Promega Corporation, Madison, WI, USA). cDNA was obtained from RNA using the high-capacity cDNA reverse transcription kit (Applied Biosystems, Foster City, CA, USA). To study the cholesterol metabolism, real-time PCR was performed using the END-1, HMGR, LDLr and Akt primers (Thermo-Fisher Scientific) as biomarkers.

The glyceraldehyde-3-phosphate dehydrogenase (GAPDH) gene (Thermo-Fisher Scientific) was used as a housekeeping gene, whose expression is constitutive in these cells. Amplification conditions in a thermocycler 7300 (Applied Biosystems, CA, USA) were universal and the quantification of



gene expression was performed in a relative way, so that the magnitude of the physiological changes in the biomarker gene was obtained in comparison with the housekeeping gene. For calculations, the formula  $2-\Delta\Delta Ct$  was used.

## 2.7. Statistical analysis

Microbiota count and SCFA concentration in culture medium were expressed as mean  $\pm$  standard deviation (SD) of the average of two replicates. Cell line results were expressed as mean  $\pm$  SD of the average of two independent studies, including 2 replicates per study ( $n = 4$ ). One-way analysis of variance (ANOVA), using Fisher's least significant difference (LSD) test, was used to determine significant differences ( $p < 0.05$ ) between data from cells incubated with culture medium before and after wine treatment. All the statistical analyses were carried out using GraphPad Prism 9 version 9.4.1 for Windows (GraphPad Software, San Diego, California, USA).

## 3. Results and discussion

The bioactivity of red wines has been associated with the presence of flavanols. In this work, two different red wines from two consecutive seasons (2020 and 2021) were subjected to a dynamic gastrointestinal digestion model, including colonic fermentation, to study the potential cardioprotective and insulin resistance effects of flavanol colonic metabolites.

### 3.1. Stability and kinetics of wine flavanols during dynamic *in vitro* gastrointestinal digestion

Absorption of dietary components occurs predominantly during gastrointestinal digestion. With only limited exceptions, the bioavailability of food phenolic compounds is low, particularly in the case of the oligomeric and polymeric forms of flavanols, such as proanthocyanidins.<sup>5</sup> Consequently, the beneficial effects attributed to the flavanol fraction of wine

appear to be primarily linked with the non-absorbed compounds that transit to the colon. To evaluate the stability of phenolic compounds during gastrointestinal digestion and, therefore, predict the amount and nature of flavanols reaching the colon, we performed simulated gastric and intestinal digestion. Interestingly, the digestion of the selected red wines from the two consecutive harvests (2020 and 2021) showed a similar trend (Table 2 and ESI Tables S2 and S5†), which validates the results. In line with data published by Tamargo *et al.* (2023),<sup>23</sup> we also observed a gradual decrease in the wine flavanol (precursors) concentration in the media throughout the dynamic *in vitro* gastrointestinal digestion, with partial and complete disappearance after the gastric and intestinal phases, respectively (Table 2). Regarding phenolic acids, the concentration of *p*-coumaric acid in the media increased after the intestinal digestion phase (Table 2). The concentration of protocatechuic acid was similar to that detected in the digestion media plus wine before digestion. While gallic acid remained largely unaffected after the gastric step, it was not detected after the intestinal digestion phase. The increase in the concentration of the *p*-coumaric acids after intestinal digestion could be related to the release of the polyphenols covalently bound to wine proteins.<sup>24</sup>

### 3.2. Flavanol kinetic metabolism in different colon segments during the dynamic colonic fermentation of wine

The kinetics of the wine flavanol colonic metabolism shows the overall progression of the precursors present in wine and the generation of their microbial metabolites during colonic fermentation (Fig. 2). Consistent with observations after the gastro-intestinal digestion, the behavior of flavanols from both the 2020 and 2021 wines showed similar trends. Both exhibited a similar qualitative profile of microbial metabolites, although there were some variations in their concentrations in the culture medium (Fig. 3A–C and ESI Tables S2 to S7†).

**Table 2** Phenolic composition of the media after the gastric and intestinal digestion of the 2020 and 2021 wines, respectively

Phenolic compound	2020 wine (mg L <sup>-1</sup> wine)				2021 wine (mg L <sup>-1</sup> wine)				
	Media + wine	Gastric digestion	Var (%)	Intestinal digestion	Media + wine	Gastric digestion	Var (%)	Intestinal digestion	Var (%)
<i>p</i> -Coumaric acid	0.50	0.40	-20	1.52	204	1.04	0.91	2.18	110
Protocatechuic acid	1.26	1.15	-9	0.96	-24	1.02	0.90	1.00	-2
Gallic acid	10.1	9.38	-7	nd	-100	14.0	13.3	-4	0.19
Catechin	4.18	3.02	-28	nd	-100	5.92	3.34	-44	0.32
Epicatechin	2.13	1.50	-30	nd	-100	2.51	1.35	-46	0.09
Gallocatechin	0.74	0.52	-30	nd	-100	1.30	0.78	-40	nd
Epigallocatechin	0.80	0.54	-33	nd	-100	0.72	0.40	-45	nd
Epigallocatechin gallate						0.04	0.07	96	nd
Procyanidin B1	7.72	4.62	-40	nd	-100	9.80	4.10	-58	0.46
Procyanidin B2	1.89	1.20	-37	nd	-100	2.43	1.21	-50	nd
Procyanidin B3	0.52	0.42	-19	nd	-100	0.55	0.29	-47	nd
Procyanidin T	0.02	0.01	-50	nd	-100	0.08	0.06	-28	nd

Results are expressed as mean ( $n = 2$ ). nd: not detected. Var: percentage of variation in the phenol concentration after gastric and intestinal digestion in relation to media + wine.



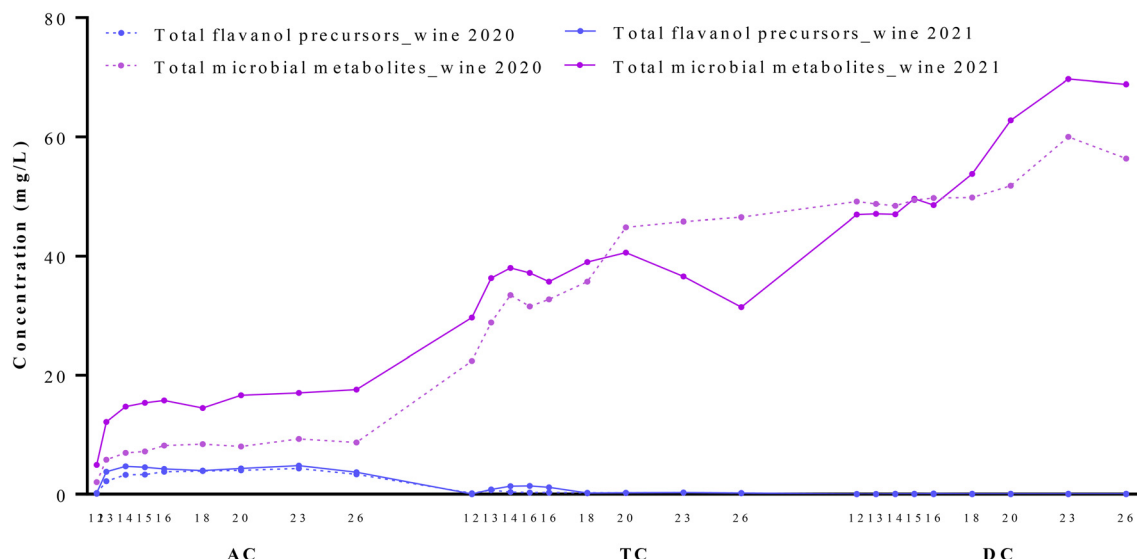


**Fig. 2** Kinetic disappearance of total flavanols (precursors) of the wines from 2020 (solid blue line) and 2021 (dashed blue line) harvests, and the parallel production of flavanol colonic metabolites (solid purple line and discontinued purple line for wines from 2020 and 2021, respectively) during the dynamic *in vitro* colonic fermentation. AC: ascending colon, TC: transversal colon, DC: descending colon. Data are expressed as mean  $\pm$  SD ( $n = 2$ ).

Based on the phenol composition of the media after the gastro-intestinal digestion (Table 2 and ESI Tables S2 and S5†), it can be inferred that no parent compounds of the wine flavanols entered the AC reactor with the exceptions of catechin, epicatechin and procyanidin B1 at very low concentrations following the digestion of the 2021 wine. However, during the early stage of colonic fermentation (AC), catechin, epicatechin, epigallocatechin, gallic acid, epigallocatechin gallate and proanthocyanidins were detected (Fig. 3A and ESI Tables S2 and S5†). The concentration of flavanols gradually decreased in TC until it completely disappeared in DC, with the exception of epigallocatechin, epigallocatechin gallate and procyanidin B1 in the 2021 wine (Fig. 3A and B). The transient disappearance of flavanols may be explained by the non-specific binding interactions of some flavonoids with lipophilic carrier proteins present in the digestion media that could be disrupted by the colonic environment or gut microbiota activity.<sup>25</sup>

The main microbial metabolites detected in the AC section were the benzoic acid related compounds: catechol, pyrogallol and gallic acid (ESI Tables S2 & S5†). The early appearance of gallic acid may result from the breakdown of more complex molecules and/or the degalloylation of the gallic acid esters of wine flavanols. Other colonic metabolites in the AC were phenyl propionic acid related compounds (Fig. 3C). This may indicate the premature microbial degradation of more complex phenolic compounds in the ascending colon.

In the TC reactor, a greater abundance and diversity of phenolic species were observed than those in the AC reactor (Fig. 3A–C). In the TC section, increases in valerolactones and valeric acids were observed. These are exclusively microbial metabolites of flavanols.<sup>7</sup> In line with the previously described microbial metabolites,<sup>7</sup> we identified di- and monohydroxy

propan-2-ol, from which hydroxylated valerolactones are generated (ESI Tables S3 & S6†). The subsequent microbial catabolism of valerolactones produces valeric acid derivatives with varying degrees of hydroxylation, and these were abundant in the TC section. Other microbial metabolites detected in the AC section, such as *p*-coumaric acid, gallic acid, pyrogallol and catechol, were also detected in the TC section at lower concentrations.

In the DC section, the predominant compounds included 5-(3,4-dihydroxy phenyl) valerolactone, 5-(3,4-dihydroxy phenyl) valeric acid, 4-hydroxy-5-(4-hydroxy phenyl) valeric acid, benzoic acid related compounds and catechol (ESI Tables S4 & S7†). The main compounds generated during the colonic fermentation in the DC section belong to the family of phenyl-propionic and phenylacetic acids, especially 3-hydroxyphenyl acetic acid and 3(4-hydroxy) phenyl propionic acid (ESI Tables S4 & S7†). This trend indicates the persistence of these compounds during colonic transit, possibly due to the continuous metabolism of wine flavanols resulting in the formation of valerolactones and valeric acids. These results are consistent with the observations made by Firman *et al.* (2020),<sup>26</sup> where the first colonic segment (AC) exhibited less diversity and abundance of phenolic species compared to TC and DC. Additionally, our findings align with the same authors' conclusion that TC and DC have closely related metabolic profiles. Similarly, a study by Cattivelli *et al.* (2023)<sup>12</sup> showed that the degradation driven by the colon microbiota of cooked red-skinned onion flavonols resulted in the accumulation of three main metabolites, *i.e.*, 3-(3'-hydroxyphenyl)propanoic acid, 3-(3'-hydroxyphenyl)acetic acid and 3-(3',4'-dihydroxyphenyl)acetic acid. This provides further evidence of significant colonic metabolism in the TC and DC sections.



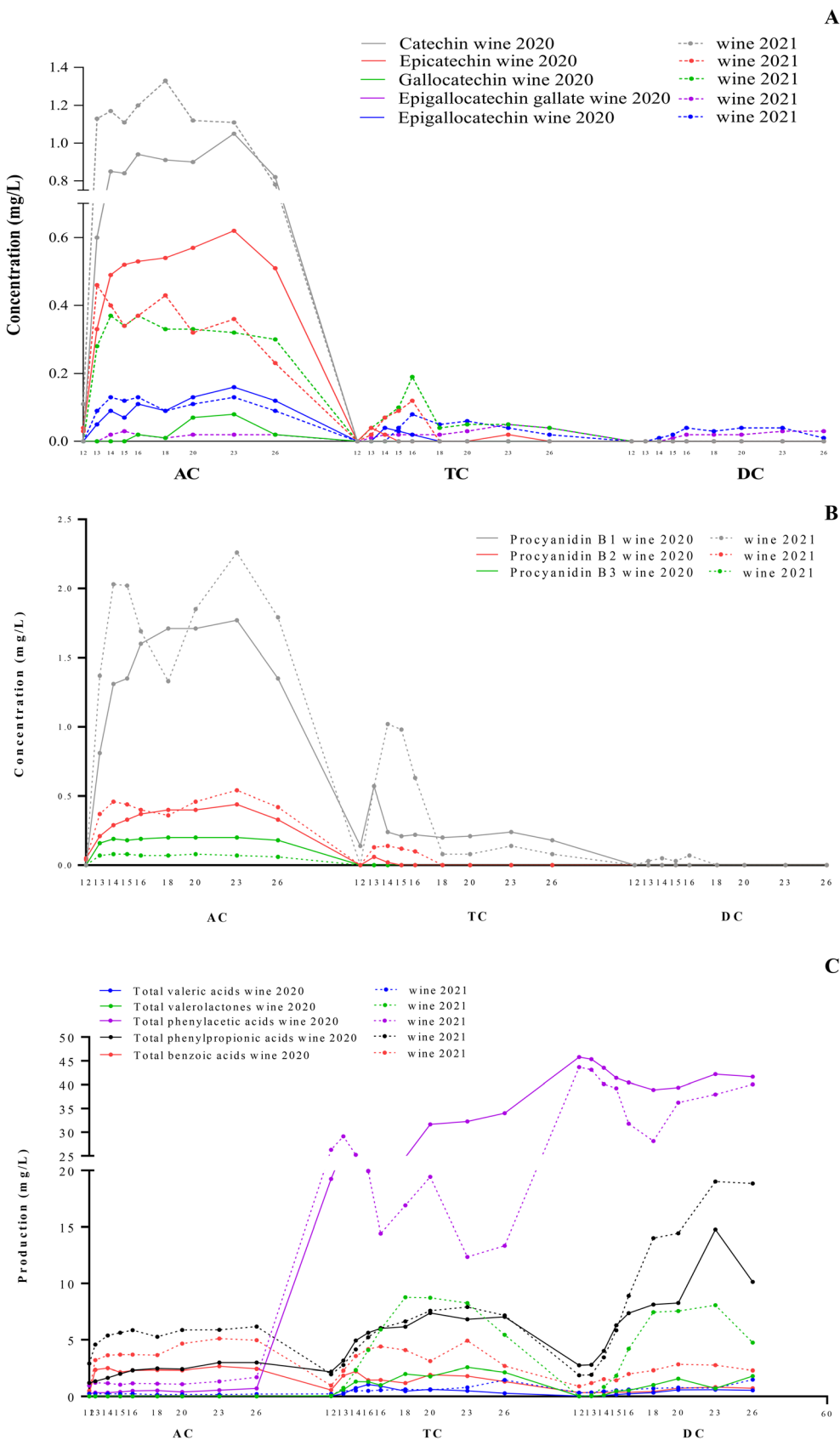


**Fig. 3** Kinetic disappearance of flavanol monomers (A) and oligomers (B) of wines from 2020 (solid line) and 2021 (dashed line) harvests, and microbial metabolite production (C) during the dynamic *in vitro* colonic fermentation. AC: ascending colon, TC: transversal colon, DC: descending colon. Data are expressed as mean  $\pm$  SD ( $n = 2$ ).



Given the crucial link between the bioavailability of dietary phenolic compounds and their efficacy as bioactive molecules, numerous *in vivo* studies have been conducted to elucidate the impact of phenolic microbial metabolites on the overall bioavailability.<sup>27</sup> Considering that flavanols represent the principal phenolic constituents in red wine, the results presented here offer important insights into the association between health benefits, particularly cardiovascular health, and the presence of colonic microbial products derived from wine flavanols. Indeed, the relevance of valerolactones and valeric acid related compounds is evidenced, as they have been proposed as intake biomarkers of food containing proanthocyanidins.<sup>27</sup>

### 3.3. Impact of wine flavanols on the microbial population and SCFA production

It has been suggested that dietary polyphenols, including those from red wine, can modulate the gut microbiota and/or their metabolic activity, positively impacting the reduction of CVD risk factors.<sup>28</sup> In this work, the plate counting technique was used to examine variations in viable gut bacteria in the media of the AC, TC and DC sections during the stabilization period (days 0, 5, 7 and 12) and during the wine treatment period (days 14, 19, 21 and 26) (Fig. 1). During the initial phase of stabilization, the fecal bacteria introduced adapted to each reactor according to the characteristics of the media, such as pH and nutrient availability.<sup>26</sup> In our study (Fig. 4), during the wine treatment period, (days 14, 19, 21 and 26), *Bifidobacterium* gradually increased in the three colon sections except in AC with the 2021 wine treatment (Fig. 4A). In contrast, the count of *Enterobacter* tended to decrease in the three reactors, which is particularly evident during the treatment

period with the 2021 wine (Fig. 4). Finally, there were no evident changes in the count of *Lactobacillus* in the AC, TC and DC sections during the treatment period with the 2021 wine; in contrast, the treatment with the 2020 wine tended to increase the bacterial population in the three reactors (Fig. 4). In contrast to the differences observed for the microbial metabolite profile of flavanols in the three reactors during colonic fermentation, no marked differences were observed in *Bifidobacterium*, *Enterobacter* and *Lactobacillus* counts between the culture media from AC, TC and DC (Fig. 4).

SCFAs are microbial products derived from the anaerobic fermentation of non-absorbed dietary compounds, especially carbohydrates and, to a lesser extent, dietary and endogenous proteins.<sup>29</sup> Chromatographic analysis of the culture media from the AC, TC and DC reactors, collected at the baseline (stabilization period, day 12) and at the end of the wine treatment period (day 26) (Fig. 1), showed that wine supplementation modulates the production rate of SCFAs (Fig. 5). In both wines (2020 and 2021), the most marked change was the increase in the production of butyric and propionic acids in the TC and DC sections (Fig. 5B & C). Regarding acetic acid, we observed that its production was stimulated during the incubation of the 2021 wine in all the reactors but not with the 2020 wine. Since acetic and butyric acids share a common metabolic pathway, it is suggested that the presence of red wine may favor the synthesis of butyric acid at the expense of acetic acid.<sup>26,29</sup> This effect on the stimulation of butyric and propionic acid production may also be due to a direct interaction of phenolic metabolites with bacterial activity or a direct interaction of these compounds in the metabolism of these SCFAs. These results are in concord with a recent study,<sup>23</sup> in which the production of butyric acid was signifi-

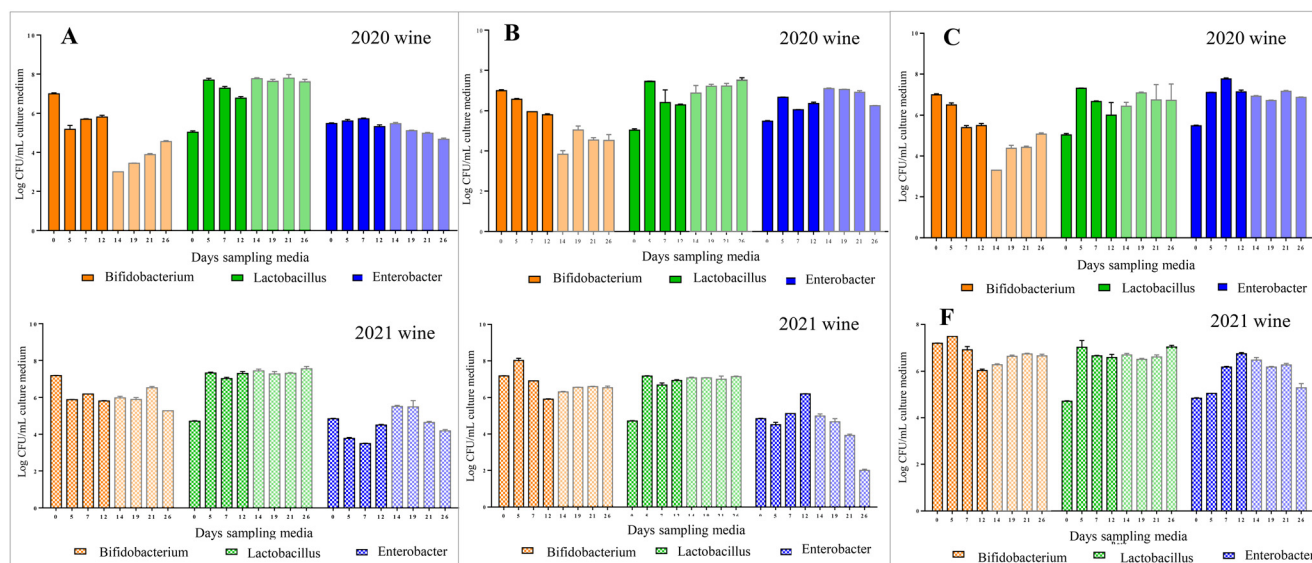


**Fig. 4** Bacterial abundance in culture medium (A) AC: ascending colon, (B) TC: transversal colon, (C) DC: descending colon, sampled at different days of the stabilization period (days 0, 5, 7 and 12 in lighter colour) and the wine treatment period (days 14, 19, 21 and 26). Wine from 2020 (solid bars) and wine from 2021 (grid fill). Data are expressed as mean  $\pm$  SD ( $n = 2$ ).



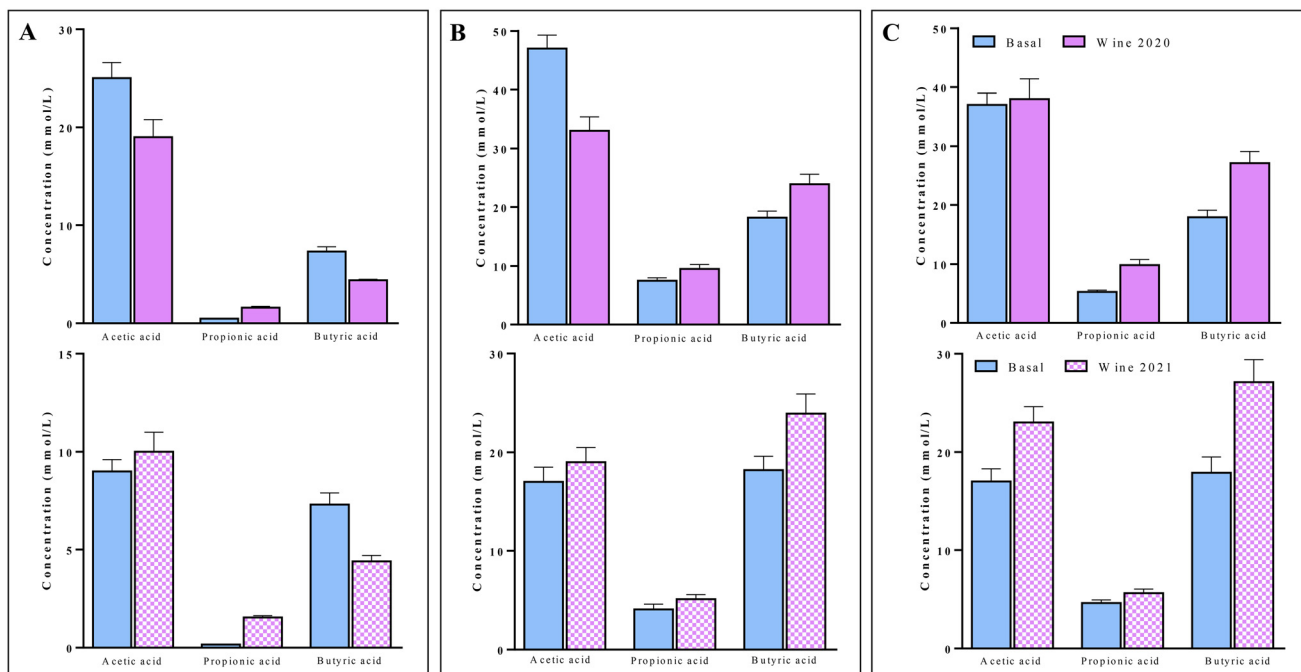


**Fig. 5** Amount of short chain fatty acids quantified in (A) AC: ascending colon, (B) TC: transversal colon and (C) DC: descending colon at the beginning (basal, day 12) and at the end of the treatment (day 26) period after the supplementation with wines from 2020 (solid bars) and 2021 (grid bars). Data are expressed as mean  $\pm$  SD ( $n = 2$ ).

cantly higher when red wine was fermented alone compared to when it was combined with a lipid food model, suggesting that the non-bioavailable fraction resulting from wine digestion could potentiate the production of butyric acid. Conversely, Suo *et al.* (2021)<sup>30</sup> did not observe differences in the generation of various SCFA classes when fermenting isolated high-molecular weight polyphenolic complexes and oligomeric phenols compared with the control (deionized water). This indicates that wine as a whole entity may play a role in the generation of butyric acid rather than isolated (poly) phenols. Extensive research has investigated the role of SCFAs in human health, with particular emphasis on butyric acid due to its significant impact on various physiological processes in the human body.<sup>31</sup>

### 3.4. Study of the potential cardioprotective activity of wine flavanol microbial metabolites in cell line models

CVDs comprise a spectrum of disorders, including coronary artery disease, stroke, hypertension and heart failure. Many researchers have identified a positive association between moderate red wine intake and an improvement in cardiovascular health parameters. Over the last decade, research has emphasized the role of the microbiome in regulating cardiovascular physiology and disease progression. These findings highlight the importance of identifying whether microbial metabolites produced from wine polyphenols contribute to the observed health effects. Understanding the interplay between wine polyphenols, the gut microbiota, and cardiovascular health could provide valuable insights into uncovering novel

therapeutic strategies aimed at preventing and managing CVDs. In order to study the cardio-protective effect of microbial metabolites, culture media from the AC, TC and DC reactors collected at the baseline (stabilization period day 12) and at the end of the wine treatment period (day 26) (Fig. 1), containing wine flavanol microbial metabolites, were exposed to endothelial and hepatic cell models.

**3.4.1. Cell viability assessment.** A fluorometric assay was performed to assess the potential toxicological impact of colonic fermentation media. Based on the cell viability assay performed on EA.hy926 endothelial and HepG2 hepatic cells treated for 24 hours with culture media from the AC, TC and DC compartments (Fig. 1), a dilution of 1/8 was selected to study the functionality of colonic metabolites as this dilution exhibited no cytotoxicity towards the cells (data not shown).

**3.4.2. Effect of wine flavanol colonic metabolites on NO levels and endothelin (END-1) expression in HepG2 cells.** Endothelial cells were utilized to assess the impact of flavanol microbial metabolites present in the three colonic culture media (AC, TC and DC) on vascular tone regulation. We focused on two key vasoactive substances released from the endothelium: nitric oxide (NO) and endothelins (ETs). While NO exerts potent vasodilatory effects, ETs are among the most potent vasoconstrictors. In the present study, we investigated the release of NO and the expression level of mRNA END-1, observing significant statistical differences between cells incubated with the stabilization media at 12 days (basal) and the wine-fermented media at 26 days (wine treatment period) ( $p < 0.05$ ) (Fig. 6). Specifically, the production of NO in cells incu-

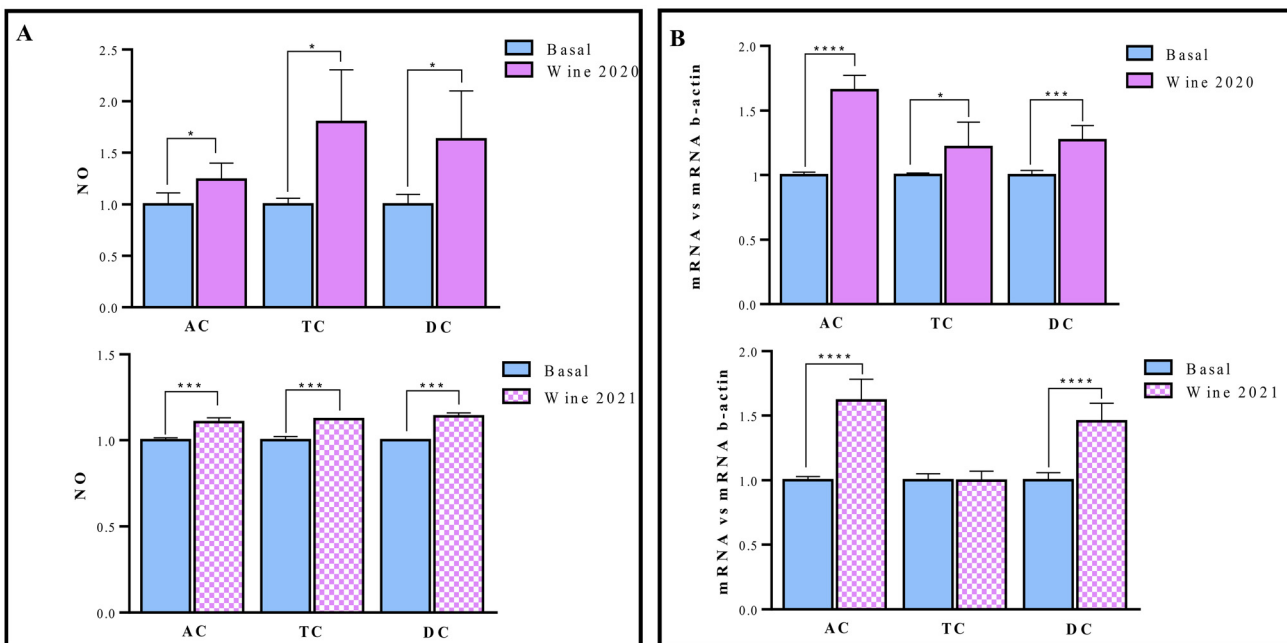


**Fig. 6** Evaluation of endothelial function parameters through (A) nitric oxide (NO) production and (B) expression levels of nitric oxide synthase (ENDT) mRNA in EA.hy926 cells exposed to media obtained from different colonic reactors representing the ascending colon (AC), transversal colon (TC) and descending colon (DC) sections, before and after 2020 wine (purple solid bars) and 2021 wine (purple grid bars) supplementation. Data are expressed as mean  $\pm$  SD ( $n = 4$ ). \* $p < 0.05$ ; \*\* $p < 0.001$ ; and \*\*\* $p < 0.0001$  with respect to the control.

bated with the media containing the microbial metabolites (wine treatment) was significantly higher than in the stabilization media (basal) in the three reactors for the 2020 and 2021 wines. The level of mRNA of ET-1 increased significantly in all the reactors, except for TC after the 2021 wine treatment (Fig. 6B). Consistent with previous research, changes in the END-1 concentration in cells demonstrated an inverse association with the NO concentration, maintaining a suitable vascular tone balance and preventing endothelial cell dysfunction.<sup>32</sup>

**3.4.3. Modulation of cholesterol metabolism and insulin resistance in HepG2 cells treated with wine flavanol colonic metabolites.** Another risk factor for cardiovascular disease is the level of lipids, particularly LDL cholesterol. Therefore, we explored the potential of the wine flavanol microbial metabolites present in the culture media from the AC, TC and DC reactors, before and after wine treatment, to influence the expression of the LDL receptor (LDLr) and HMG-CoA in the hepatic cell line, both of which are involved in cholesterol biosynthesis. This study revealed that the culture media collected from the three reactors during both wine treatments (2020 and 2021) can enhance the expression level of mRNA LDLr (Fig. 7A), thereby facilitating the removal of LDL cholesterol from circulation.<sup>33</sup> This effect can be attributed to the presence of several wine flavanol microbial metabolites in the culture media.

The regulation in the expression of mRNA HMGCoA showed differences between the wine from 2020 and that from 2021 (Fig. 7B). In this instance, only cells exposed to the culture media from the TC and DC sections treated with the 2021 wine showed a significant down-regulation in the

expression of mRNA HMGCo-A, contributing to the inhibitory effect of cholesterol biosynthesis in the liver. Previous research has found an inverse relationship between the mRNA abundance of HMG-CoA reductase and LDLr mRNA.<sup>34</sup> These results suggest that microbial metabolites generated by colonic fermentation of wine flavanols stimulate the expression of the LDLr gene (Fig. 7A), whereas transcript levels of HMG-CoA were not significantly affected by the wine treatment (Fig. 7B), and these may depend on the concentration of microbial metabolites rather than the composition.

Regarding insulin resistance, a risk in CVD, the liver plays a pivotal role in regulating blood glucose levels through various processes including gluconeogenesis, glycogen synthesis, and glycogen breakdown. AKT, a key mediator in the PI3K/AKT signaling pathway, exerts influence over these metabolic processes. Reduced AKT levels can hinder glucose transportation and disrupt glycogen synthesis, potentially resulting in elevated blood glucose levels and insulin resistance.<sup>35</sup> In the present study, the hepatic cells exposed to the culture media from the AC, TC and DC reactors from microbial fermentation of the 2020 and 2021 wines reduced the risk of insulin resistance, disrupting glycogen synthesis (Fig. 8A) and inhibiting hepatic glucose generation by down-regulation of mRNA AKT expression (Fig. 8B). These findings suggest that wine flavanol microbial metabolites can modulate hepatic glucose metabolism, thereby potentially offering therapeutic benefits in managing insulin resistance and glycemic control. In addition to microbial metabolites, the SCFAs present in the fermentation culture media (from AC, TC and DC) could modulate the

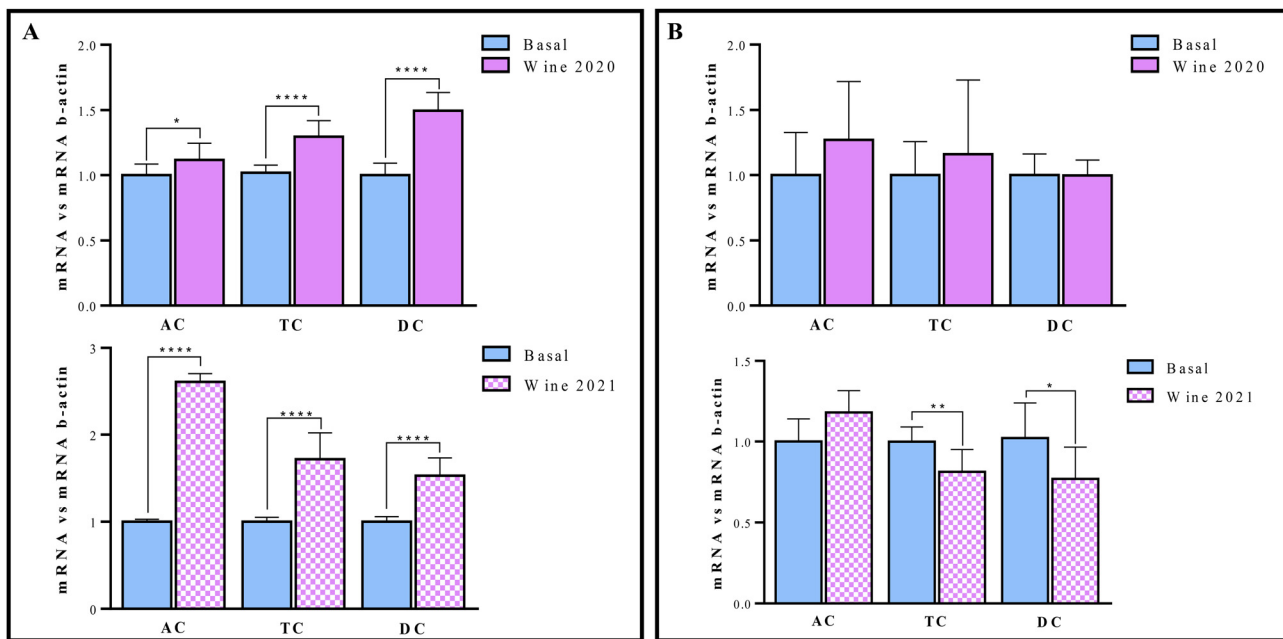


**Fig. 7** Cholesterol metabolism evaluated by the expression levels of (A) LDL receptor mRNA and (B) HMGCo-R mRNA in HepG2 cells exposed to media obtained from different colonic reactors representing the ascending colon (AC), transversal colon (TC) and descending colon (DC) before and after 2020 wine (purple solid bars) and 2021 wine (purple grid bars) supplementation. Data are expressed as mean  $\pm$  SD ( $n = 4$ ). \* $p < 0.05$ ; \*\* $p < 0.005$ ; and \*\*\*\* $p < 0.0001$  with respect to the control.

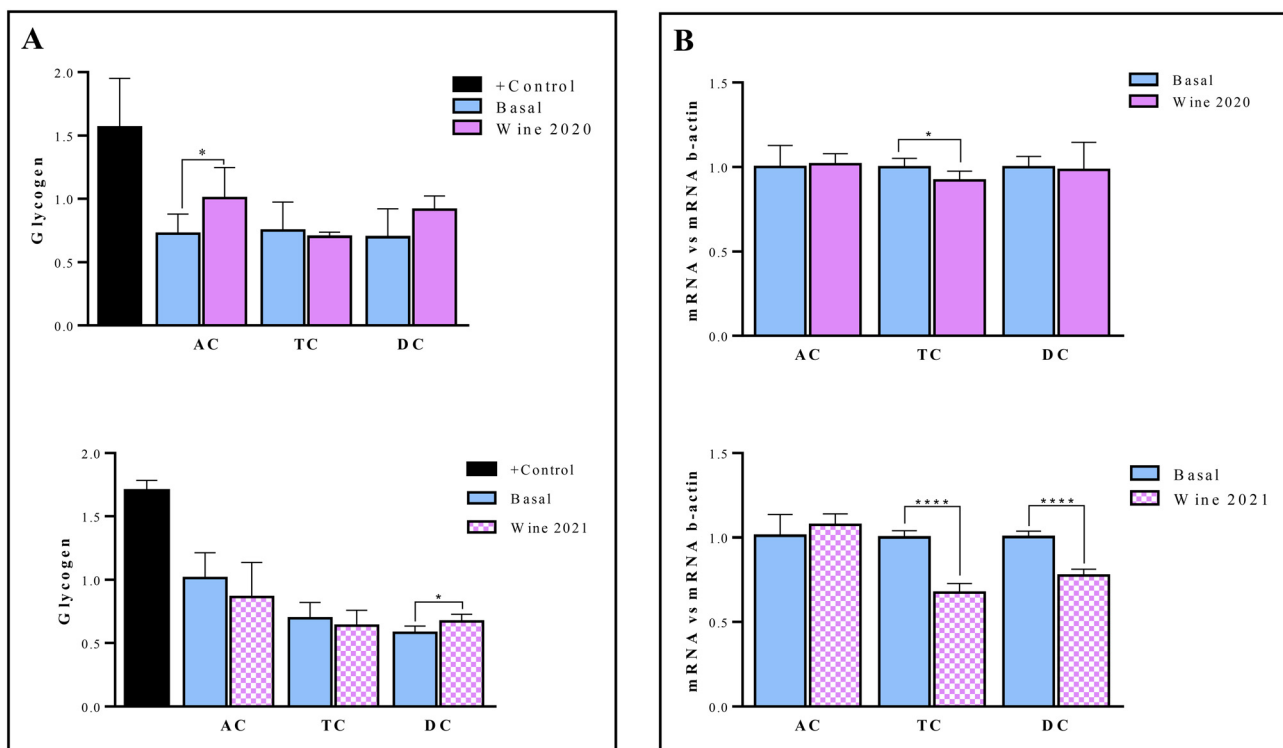


**Fig. 8** Carbohydrate metabolism evaluation by (A) synthesis of glycogen and (B) expression levels of Akt mRNA in HepG2 cells exposed to media obtained from different colonic reactors representing the ascending colon (AC), transversal colon (TC) and descending colon (DC) before and after 2020 wine (purple solid bars) and 2021 wine (purple grid bars) supplementation. Data are expressed as mean  $\pm$  SD ( $n = 4$ ). \* $p < 0.05$  and \*\*\*\* $p < 0.0001$  with respect to the control.

CVD risk parameters studied. Previous data showed that butyric acid modulates insulin resistance and the accumulation of fat in the liver.<sup>11</sup> In addition, the increment in the plasma levels of butyric acid has been associated with an improvement of the endothelial function.<sup>36</sup>

In conclusion, the results of the present study show that wine flavanols, subjected to a dynamic *in vitro* digestion model, reach the colon where they are transformed by the colonic microbiota. The colonic fermentation of wine flavanols resulted in the accumulation of three main metabolites, *i.e.*, 3-(3'-hydroxyphenyl)propanoic acid, 3-(3'-hydroxyphenyl)acetic acid and 3-(3',4'-dihydroxyphenyl)acetic acid. In addition, an increase in a complex mixture of valerolactone and valeric acid derivatives was observed in the TC and DC sections. In parallel, a significant increase in the production of butyric and propionic acids was observed in the TC and DC sections, respectively, as well as an increase in the count of certain bacteria, mainly *Bifidobacterium*. The functionality study shows that exposing fermentation media containing wine flavanol microbial metabolites to endothelial and hepatic cell lines positively modulates four biomarkers associated with three CVD risk factors. Specifically, an increase was observed in the vasodilator NO that improves the blood pressure. In addition, there was an improvement in the LDL receptors and the HMGCoA enzyme, with a positive effect on cholesterol metabolism, and the reduction of glycogen levels improving insulin resistance. The results of this study reinforce the idea that wine flavanols are intensively metabolised by the colonic microbiota to generate a complex mixture of their bioactive forms that could influence host health.

## Author contributions

Juana Mosele: formal analysis, investigation, writing – original draft, and writing – review & editing; Blanca Viadel: conceptualization, project administration, validation, data curation, formal analysis, investigation, methodology, and software; Silvia Yuste: formal analysis, investigation, and methodology; Lidia Tomás-Cobos: formal analysis, investigation, and methodology; Sandra García-Benlloch: formal analysis, investigation, and methodology; María-Teresa Escribano Bailón: conceptualization, data curation, formal analysis, and investigation; Ignacio García Estévez: conceptualization, data curation, formal analysis, and investigation; Pilar Moretón Fraile: conceptualization, funding acquisition, and project administration; Fernando Rodríguez de Rivera: conceptualization, funding acquisition, and project administration; Soledad de Domingo Casado: conceptualization, funding acquisition, and project administration; María-José Motilva: investigation, methodology, writing – original draft, and writing – review & editing.

## Data availability

The data supporting this article have been included as part of the ESI (Fig. S1 and Tables S1–S7).†

## Conflicts of interest

On behalf of all the authors, the corresponding author states that there is no conflict of interest.

## Acknowledgements

This study was supported by the MCIN (Ministerio de Ciencia e Innovación) through the CDTI project IDI-20210434. Silvia Yuste has a Margarita Salas postdoctoral grant funded by the European Union-NextGenerationEU through the Ministerio de Universidades and the Universitat de Lleida. The authors are grateful to the technical staff of the Instrumental Analysis Service at the ICVV for their UHPLC-QqQ-MS/MS analytical support.

## References

- 1 R. G. Ntuli, Y. Saltman, R. Ponangi, D. W. Jeffery, K. Bindon and K. L. Wilkinson, Impact of fermentation temperature and grape solids content on the chemical composition and sensory profiles of Cabernet Sauvignon wines made from flash détente treated must fermented off-skins, *Food Chem.*, 2022, **369**, 130861.
- 2 I. Buljeta, A. Pichler, J. Šimunović and M. Kopjar, Beneficial Effects of Red Wine Polyphenols on Human Health: Comprehensive Review, *Curr. Issues Mol. Biol.*, 2023, **45**, 782–798.
- 3 X. Zhang, X. Song, X. Hu, F. Chen and C. Ma, Health benefits of proanthocyanidins linking with gastrointestinal modulation: An updated review, *Food Chem.*, 2022, 134596.
- 4 G. Raman, M. Shams-White, E. E. Avendano, F. Chen, J. A. Novotny and A. Cassidy, Dietary intakes of flavan-3-ols and cardiovascular health: a field synopsis using evidence mapping of randomized trials and prospective cohort studies, *Syst. Rev.*, 2018, **7**, 100.
- 5 F. Castello, G. Costabile, L. Bresciani, M. Tassotti, D. Naviglio, D. Luongo, P. Ciciola, M. Vitale, C. Vetrani, G. Galaverna, F. Brighenti, R. Giacco, D. Del Rio and P. Mena, Bioavailability and pharmacokinetic profile of grape pomace phenolic compounds in humans, *Arch. Biochem. Biophys.*, 2018, **646**, 1–9.
- 6 S. Yuste, I. A. Ludwig, L. Rubió, M.-P. Romero, A. Pedret, R.-M. Valls, R. Solà, M.-J. Motilva and A. Macià, In vivo bio-transformation of (poly) phenols and anthocyanins of red-fleshed apple and identification of intake biomarkers, *J. Funct. Foods*, 2019, **55**, 146–155.
- 7 J. I. Mosele, A. Macià, M. P. Romero, M. J. Motilva and L. Rubió, Application of *in vitro* gastrointestinal digestion and colonic fermentation models to pomegranate products (juice, pulp and peel extract) to study the stability and catabolism of phenolic compounds, *J. Funct. Foods*, 2015, **14**, 529–540.



8 M. J. Cires, P. Navarrete, E. Pastene, C. Carrasco-Pozo, R. Valenzuela, D. A. Medina, M. Andriamihaja, M. Beaumont, F. Blachier and M. Gotteland, Effect of a proanthocyanidin-rich polyphenol extract from avocado on the production of amino acid-derived bacterial metabolites and the microbiota composition in rats fed a high-protein diet, *Food Funct.*, 2019, **10**, 4022–4035.

9 M. Monagas, M. Urpi-Sarda, F. Sánchez-Patán, R. Llorach, I. Garrido, C. Gómez-Cordovés, C. Andres-Lacueva and B. Bartolome, Insights into the metabolism and microbial biotransformation of dietary flavan-3-ols and the bioactivity of their metabolites, *Food Funct.*, 2010, **1**, 233–253.

10 M. A. Polewski, D. Esquivel-Alvarado, N. S. Wedde, C. G. Kruger and J. D. Reed, Isolation and characterization of blueberry polyphenolic components and their effects on gut barrier dysfunction, *J. Agric. Food Chem.*, 2019, **68**, 2940–2947.

11 X. Zhao, Y. Wu, H. Liu, N. Hu, Y. Zhang and S. Wang, Grape seed extract ameliorates PhIP-induced colonic injury by modulating gut microbiota, lipid metabolism, and NF-κB signaling pathway in rats, *J. Funct. Foods*, 2021, **78**, 104362.

12 A. Cattivelli, L. Nissen, F. Casciano, D. Tagliazucchia and A. Gianotti, Impact of cooking methods of red-skinned onion on metabolic transformation of phenolic compounds and gut microbiota changes, *Food Funct.*, 2023, **14**, 3509–3525.

13 L. Nissen, A. Cattivelli, F. Casciano, A. Gianotti and D. Tagliazucchi, Roasting and frying modulate the phenolic profile of dark purple eggplant and differently change the colon microbiota and phenolic metabolites after *in vitro*, digestion and fermentation in a gut model, *Food Res. Int.*, 2022, **160**, 111702.

14 R. A. Kemperman, S. Bolca, L. C. Roger and E. E. Vaughan, Novel approaches for analysing gut microbes and dietary polyphenols: challenges and opportunities, *Microbiology*, 2010, **156**, 3224–3231.

15 I. García-Estevez, C. Alcalde-Eon and M. T. Escribano-Bailón, Flavanol quantification of grapes via multiple reaction monitoring mass spectrometry. application to differentiation among clones of *Vitis Vinifera* L. cv Rufete grapes, *J. Agric. Food Chem.*, 2017, **65**, 6359–6368.

16 J. A. Nieto, C. Rosés, P. García-Ibáñez, B. Pérez, B. Viadel, A. Romo-Hualde, F. I. Milagro, A. Barceló, M. Carvajal, E. Gallego and A. Agudelo, Fiber from elicited butternut pumpkin (*Cucurbita moschata* D. cv. Ariel) modulates the human intestinal microbiota dysbiosis, *Int. J. Biol. Macromol.*, 2024, **269**(Pt 2), 132130.

17 P. Marteau, B. Flourié, P. Pochard, C. Chastang, J. F. Desjeux and J. C. Rambaud, Effect of the microbial lactase (EC 3.2.123) activity in yoghurt on the intestinal absorption of lactose: An *in vivo* study in lactase-deficient humans, *Br. J. Nutr.*, 1990, **64**, 71–79.

18 C. Rosés, B. Viadel, J. A. Nieto, L. Soriano-Romaní, A. Romo-Hualde, A. Agudelo, F. I. Milagro and A. Barceló, Gut microbiota modulatory capacity of *Brassica oleracea italica* x *alboglabra* (Bimi®), *Food Biosci.*, 2023, **55**, 103006.

19 C. Roses, J. A. Nieto, B. Viadel, E. Gallego, A. Romo-Hualde, S. Streitenberger, F. I. Milagro, A. Barceló, E. F. Vieira and C. Soares, An *in vitro* protocol to study the modulatory effects of a food or biocompound on human gut microbiome and metabolome, *Foods*, 2021, **10**, 3020.

20 K. Molly, M. Vande Woestyne, I. De Smet and W. Verstraete, Validation of the Simulator of the Human Intestinal Microbial Ecosystem (SHIME) Reactor Using Microorganism-Associated Activities, *Microb. Ecol. Health Dis.*, 1994, **7**, 191–200.

21 K. Molly, M. Vande Woestyne and W. Verstraete, Development of a 5-Step Multi-Chamber Reactor as a Simulation of the Human Intestinal Microbial Ecosystem, *Appl. Microbiol. Biotechnol.*, 1993, **39**, 254–258.

22 C. Royo, Y. Ferradás, J. M. Martínez-Zapater and M. J. Motilva, Characterization of Tempranillo negro (VN21), a high phenolic content grapevine Tempranillo clone, through UHPLC-QqQ-MS/MS polyphenol profiling, *Food Chem.*, 2021, **360**, 130049.

23 A. Tamargo, D. G. de Llano, C. Cuevas, J. N. Del Hierro, D. Martin, N. Molinero, B. Bartolomé and V. Moreno-Arribas, Deciphering the interactions between lipids and red wine polyphenols through the gastrointestinal tract, *Food Res. Int.*, 2023, **165**, 112524.

24 J. Liang, S. Yang, Y. Liu, H. Li, M. Han and Z. Gao, Characterization and stability assessment of polyphenols bound to *Lycium barbarum*, polysaccharide: Insights from gastrointestinal digestion and colon fermentation, *Food Res. Int.*, 2024, **179**, 114036.

25 P. M. Joyner, Protein Adducts and Protein Oxidation as Molecular Mechanisms of Flavonoid Bioactivity, *Molecules*, 2021, **26**, 5102.

26 J. Firman, L. Liu, C. Tanes, E. S. Friedman, K. Bittinger, S. Daniel, P. van den Abbeele and B. Evans, Metabolic Analysis of Regionally Distinct Gut Microbial Communities Using an *In Vitro* Platform, *J. Agric. Food Chem.*, 2020, **68**, 13056–13067.

27 P. Mena, I. A. Ludwig, V. B. Tomatis, A. Acharjee, L. Calani, A. Rosi, F. Brighenti, S. Ray, J. L. Griffin, L. J. Bluck and D. Del, Rio. Inter-individual variability in the production of flavan-3-ol colonic metabolites: preliminary elucidation of urinary metabotypes, *Eur. J. Nutr.*, 2019, **58**, 1529–1543.

28 W. H. W. Tang, F. Bäckhed, U. Landmesser and S. L. Hazen, Intestinal Microbiota in Cardiovascular Health and Disease: JACC State-of-the-Art Review, *J. Am. Coll. Cardiol.*, 2019, **73**, 2089–2105.

29 S. Macfarlane and G. T. Macfarlane, Regulation of short-chain fatty acid production, *Proc. Nutr. Soc.*, 2003, **62**, 67–72.

30 H. Suo, M. R. I. Shishir, J. Xiao, M. Wang, F. Chen and K. W. Cheng, Red Wine High-Molecular-Weight Polyphenolic Complex: An Emerging Modulator of Human Metabolic Disease Risk and Gut Microbiota, *J. Agric. Food Chem.*, 2021, **69**, 10907–10919.



31 D. J. Morrison and T. Preston, Formation of short chain fatty acids by the gut microbiota and their impact on human metabolism, *Gut Microbes*, 2016, **7**, 189–200.

32 S. Kuruppu, N. W. Rajapakse, R. A. Dunstan and A. I. Smith, Nitric oxide inhibits the production of soluble endothelin converting enzyme-1, *Mol. Cell. Biochem.*, 2014, **396**, 49–54.

33 K. Ioriya, K. Kino, S. Horisawa, T. Nishimura, M. Muraoka, T. Noguchi and N. Ohashi, Pharmacological profile of SMP-797, a novel acyl-coenzyme a: cholesterol acyltransferase inhibitor with inducible effect on the expression of low-density lipoprotein receptor, *J. Cardiovasc. Pharmacol.*, 2006, **47**, 322–329.

34 I. J. Cho, J. Y. Ahn, S. Kim, M. S. Choi and T. Y. Ha, Resveratrol attenuates the expression of HMG-CoA reductase mRNA in hamsters, *Biochem. Biophys. Res. Commun.*, 2008, **367**, 190–194.

35 M. Li, X. Chi, Y. Wang, S. Setrerrahmane, W. Xie and H. Xu, Trends in insulin resistance: insights into mechanisms and therapeutic strategy, *Signal Transduction Targeted Ther.*, 2022, **7**, 216.

36 Q. Tian, F. P. Leung, F. M. Chen, X. Y. Tian, Z. Chen, G. Tse, S. Ma and W. T. Wong, Butyrate protects endothelial function through PPAR $\delta$ /miR-181b signaling, *Pharmacol. Res.*, 2021, **169**, 105681.

